



Global distribution of CO₂ in the Upper-Troposphere and Stratosphere

M. Diallo^{1,2}, B. Legras¹, E. Ray^{3,4}, A. Engel⁵, and J. A. Añel^{2,6}

¹Laboratoire de Météorologie Dynamique, UMR8539, IPSL, UPMC/ENS/CNRS/Ecole Polytechnique, Paris, France

²EPhysLab, Facultad de ciencias, Universidade de Vigo, Ourense, Spain

³Chemical Sciences Division, Earth Systems Research Laboratory, NOAA, Boulder, Colorado, USA

⁴Cooperative Institute for Research in Environmental Sciences, University of Colorado, Boulder, Colorado, USA

⁵Institute for Atmospheric and Environmental Sciences, Goethe University Frankfurt, Frankfurt am Main, Germany

⁶Smith School of Enterprise and the Environment, University of Oxford, Oxford, UK

Correspondence to: M. Diallo (mdiallo@lmd.ens.fr)



Abstract

In this study, we aim to reconstruct a relevant and new database of monthly zonal mean distribution of *carbon dioxide* (CO_2) at global scale extending from the *upper-troposphere* (UT) to *stratosphere* (S). This product can be used for model and satellite validation in the UT/S, as a prior for inversion modelling and mainly to analyse a plausible feature of the stratospheric-tropospheric exchange as well as the stratospheric circulation and its variability. To do so, we investigate the ability of a Lagrangian trajectory model guided by ERA-Interim reanalysis to construct the CO_2 abundance in the UT/S. From 10 year backward trajectories and tropospheric observations of CO_2 , we reconstruct upper-tropospheric and stratospheric CO_2 over the period 2000–2010. The inter-comparisons of the reconstructed CO_2 with mid-latitude vertical profiles measured by balloon samples as well as quasi-horizontal air samples from ER-2 aircraft during SOLVE and CONTRAIL campaigns exhibit a remarkable agreement. That demonstrates the potential of Lagrangian model to reconstruct CO_2 in the UT/S. The zonal mean distribution exhibits relatively large CO_2 in the tropical stratosphere due to the seasonal variation of the tropical upwelling of Brewer-Dobson circulation. During winter and spring, the *tropical pipe* is relatively isolated but is less confined during summer and autumn so that high CO_2 values are more readily transported out of the tropics to the mid- and high latitude stratosphere. The shape of the vertical profiles suggests that relatively high CO_2 above 20 km altitude mainly enter the stratosphere through tropical upwelling. CO_2 mixing ratio is relatively low in the polar and tropical regions above 25 km. On average the CO_2 mixing ratio decreases with altitude by 6–8 ppmv from the UT to stratosphere (e.g. up to 35 km) and is nearly constant with altitude.

1 Introduction

Over the last twenty years, climate change has made the stratosphere a focus of several debates among the scientific community. The global stratospheric meridional circulation, also called *Brewer-Dobson circulation* (BDC), has been recognized as a major component of the climate system, which affects radiative forcing (Lacis et al., 1990; Forster and Shine, 1997; Forster



et al., 2007) and atmospheric circulation (Andrews et al., 1987; Holton et al., 1995; Salby and Callaghan, 2005, 2006). The increase of the greenhouse gases, in particular *carbon dioxide* (CO₂) concentration, increases the tropical upwelling mass flux (Butchart et al., 2010; Garny et al., 2011; Abalos et al., 2015) and therefore changes the BDC.

5 CO₂ is a good tracer of the atmospheric dynamics and transport because of its long lifetime in the atmosphere where it has essentially no sources or sinks and as it is chemically inert in the free troposphere. The only stratospheric source of CO₂ is a small contribution from methane (CH₄) oxidation that is on the order of 1 ppmv (i.e. parts per million in volume) (Boucher et al., 2009). CO₂ is regularly exchanged between these four reservoirs: among
10 the biosphere (photosynthesis and respiration), lithosphere (soil and fossil pool), hydrosphere (surface and deep ocean), and atmosphere with a time residency much longer in the ocean and soil than in the atmosphere. These exchanges are described as the carbon cycle. Clearly, the increase of the anthropogenic emissions, deforestation and biomass and fossil fuel burning have systematically increased the mean CO₂ growth rate and modified its season cycle during these
15 last two decades (Tans and Keeling, 2015). With steady growth and seasonal variation, CO₂ contains a double time signature: (a) monotonically increasing and (b) periodic tracer signal that represents stringent tests of stratospheric transport and *Stratosphere-Troposphere Exchange* (STE) in models (Waugh and Hall, 2002; Bönisch et al., 2008, 2009).

20 Despite its potential to increase global warming by cooling the stratosphere and warming the troposphere, until recently, our knowledge of stratospheric CO₂ abundances and variability was sparse. In recent years several *in situ* aircraft and balloon campaigns were held to measure a number of chemical tracers including CO₂. The *in situ* campaigns included SPURT aircraft measurements in the *upper-troposphere and lower stratosphere* (UTLS) (Engel et al., 2006; Gurk et al., 2008), CONTRAIL (Sawa et al., 2008) and CARIBIC (Schuck et al., 2009; Sprung
25 and Zahn, 2010). Although sporadic in time and space coverage, these *in situ* measurements have been used to analyse the BDC changes (Andrews et al., 2001a; Engel et al., 2009; Ray et al., 2014), to validate Chemistry-Transport Models (CTMs) (Strahan et al., 2007; Waugh, 2009) and to diagnose STE (Strahan et al., 1998; Bönisch et al., 2009, 2011). The *in situ* campaigns, such as SPURT, were used in previous studies to diagnose the eddy diffusivity in



the *lowermost stratosphere* (LMS) using a 2D-advection-diffusion model (Hegglin et al., 2005) and also to quantify different transport pathways contributing to the composition of the LMS over Europe (Hoor et al., 2005, 2010). These studies helped to evolve our understanding on a finite chemical transition layer in the extra-tropical tropopause layer and identified potential gaps in our understanding. The stratospheric overworld circulation changes that affect the extra-tropical UTLS was recently assessed from balloon long-term measurements of stratospheric age tracers, such as SF₆ and CO₂. The stratospheric mean *age of air* (AoA), that is defined as the time residence of air parcels in the stratosphere (Li and Waugh, 1999; Waugh and Hall, 2002; Butchart et al., 2010), was calculated by Ray et al. (2014) more consistently from the *in situ* profile measurements of trace gases with an idealized model to identify the natural variability in the BDC and its significant linear trends. This study exhibited the importance of reconstructed *in situ* measurements to help validate the stratospheric portion of global CTMs and Chemistry Climate Models (CCMs).

In addition to the *in situ* observations that are high resolution and very localised, a large spatial and temporal coverage of CO₂ is obtained from space by satellite observations from vertical nadir sounders TOVS (Chedin et al., 2002a,b, 2003b), AIRS (Chedin et al., 2003a), SCIAMACHY (Bowman et al., 2000), IASI (Chedin et al., 2003a), GOSAT (Hammerling et al., 2012; Liu et al., 2014) and recently OCO-2 (Frankenberg et al., 2015). Chedin et al. (2003a) showed that upper air CO₂ can be retrieved from observations of TOVS, whose main mission is to measure atmospheric temperature and moisture at global scale. Foucher et al. (2009, 2011) have obtained five years of monthly mean CO₂ vertical profiles by analysing the ACE-FTS data (Bernath et al., 2005). This space-borne instrument is passive because it uses the sunset and sunrise to measure the atmospheric chemistry species, such as isotopologues, in limb-view. The main isotopologue ¹²C¹⁶O₂ passively measured in limb-view was used to retrieve the mean CO₂ in the 10–25 km altitude range. When the main isotopologue lines saturate at low altitude range from 5 to 15 km, the ¹⁸O¹⁶O isotopologue was used (more detail about the inversion approach is found in Foucher et al. (2009)). The ACE-retrieved CO₂ has shown a good agreement after its qualitatively validation with *in situ* observations for 2004–2008 time period and at the 50°N–60°N latitude bins. The ACE-FTS retrieval approach limitation was due to the dif-



5 difficulty to have an accurate high sensitivity of N_2 continuum absorption, which allows to obtain a better tangent height retrieval. The observations from space-borne instruments are oftentimes hampered by the fact that these instruments measure an integrated column, which can not be used to better understand the CO_2 distribution mechanisms. The CO_2 column measurements, essentially weighted from the middle to upper-troposphere, are also weak and not easy to interpret globally. Because of these limitations in the observations, the CTMs and Lagrangian transport models combined with these observations are a useful and complementary framework to widely diagnose the BDC and to represent the global transport and distribution of long-lived species, such as CO_2 , within the UT/S.

10 Previous studies using the two-dimensional CTM Caltech/JPL (Shia et al., 2006) and the three-dimensional CTM TM5 (Transport Model 5) (Bönisch et al., 2008) were unable to accurately represent the BDC. Bönisch et al. (2008) investigated the UTLS exchanges in a three-dimensional transport model using the observed CO_2 and SF_6 distributions and concluded that major problems occur in winter, where a too strong BDC leads to some overestimates of the CO_2 , and in boreal summer, where a too weak vertical transport arise in the UT. During autumn, the models showed a persistent reverse gradient in the lower stratosphere due to an unrealistic BDC and during spring, the transport processes through the tropical tropopause are overestimated, which explained the high CO_2 values in the lower stratosphere. Furthermore, many three-dimensional models are too diffusive and/or have too strong mixing when crossing the tropopause that lead to an underestimation of the amplitude of the seasonal cycle in the column of CO_2 (Olsen and Randerson, 2004). Shia et al. (2006) suggested that the model's lack of realistic stratospheric influence on the CO_2 could explain part of this discrepancy. The persistence of the inverted CO_2 gradient noted in these models can result in an underestimation of the exchange of air masses from the stratosphere to the troposphere in mid-latitudes during fall. Models also fail to simulate a realistic CO_2 seasonal cycle and STE because also of short time period of simulation. Shia et al. (2006) concluded that at least three years are required for the surface CO_2 to be transported into upper-troposphere and LMS then moved to the temperate and polar latitudes. In order to eliminate diffusivity effect, Lagrangian or quasi-Lagrangian model, such as CLaMS and TRACZILLA, have been widely used to investigate the transport



problem. The combination of these Lagrangian models with *in situ* observations to reconstruct chemical tracer gas significantly contributed to evolve our understanding on quantifying mixing effect to STE across the extra-tropical tropopause (Hoor et al., 2004; Pan et al., 2006; James and Legras, 2009), on analysis of the filamentary structures in both long-lived and chemically active species near the edge of the polar vortex (Konopka et al., 2003), on evaluating of the transport of carbon monoxide and long-lived trace species from the tropical troposphere to stratosphere (Pommrich et al., 2014) and finally on quantifying the processes that control UTLS composition (Riese et al., 2012).

The small scale variability in the chemical tracer gas, particularly CO₂ here, its strong gradients across the tropopause and its scarcity suitable for validation purposes lead to a challenging task for its validation in the UTLS as well as for CTMs and CCMs to reproduce well its feature (Hegglin et al., 2008).

In this paper our goal is to reconstruct a new relevant database of monthly zonal mean distribution of CO₂ at global scale extending from the upper-troposphere to stratosphere using a Lagrangian model guided by ERA-Interim reanalysis. This product can be used to validate CTMs, CCMs, as a prior for inversion modelling and mainly to analyse a plausible feature of the stratospheric-tropospheric exchange as well as the stratospheric circulation and its variability.

To do so, here, we reconstruct a global distribution of CO₂ calculated over the time period 2000-2010 from a Lagrangian transport model driven by the most recent reanalysed winds and heating rates from the ERA-Interim reanalysis of the European Centre for Medium Range Weather Forecast (ECMWF). The global distribution of CO₂ and its transport in the UT/S are investigated using backward deterministic trajectories, which are integrated over 10 years in time. We describe the method and data used in this study in Sect. 2 and Sect. 3, respectively. The reconstruction techniques of the *in situ* balloon and aircraft observations are detailed in Sect. 4. The reconstructed CO₂ are compared with observations in Sect. 5. The time series in the northern hemisphere over 10° of latitudes bins are presented in Sect. 5.3. The global monthly distribution of the zonal mean CO₂ and its variability are discussed in Sect. 6. Finally, section 7 provides further discussions and conclusions.



2 Backward trajectory method

Backward deterministic trajectories are calculated using the Lagrangian transport model (Legras et al., 2005), which is a modified version of FLEXPART (Stohl et al., 2005). TRACZILLA uses analysed winds to move particles in the horizontal direction and performs direct interpolation from data on hybrid levels. In the vertical direction, it uses either pressure coordinate and La-
5 grangian pressure tendencies, or potential temperature coordinate and heating rates. We denote the trajectories as *adiabatic* following a convention established by Eluszkiewicz et al. (2000). At each level in the vertical, air particles are initialised over a longitude-latitude grid with 2° resolution in latitude and an almost uniform spacing in longitude of $2^\circ/\cos(\phi)$, where ϕ is the
10 latitude, generating 10 255 particles on each level from pole to pole. To avoid interpolation errors, the vertical levels of the initial grid are chosen to be the hybrid levels of the ECMWF model. In order to encompass the whole stratosphere at any latitude, the 30 levels from about 400 hPa (varying according to the surface pressure) to 2 hPa are selected. Trajectories starting below the tropospheric boundary condition, which is defined as the level at which we assign
15 the free tropospheric CO_2 to air particles, are immediately stopped and therefore do not induce any computational cost. Particles starting in the stratosphere are integrated backward in time until they cross the tropopause, defined as the lower envelope of the surfaces $\theta=380$ K and $|P|=2 \times 10^{-6} \text{ K kg}^{-1} \text{ m}^2 \text{ s}^{-1}$ where P is the Ertel potential vorticity (see Sect. 4.1) and reach our tropospheric boundary condition. Ensembles of particles were launched at the end of every
20 month over the period 2000–2010 and were integrated backwards for 10 years (Diallo et al., 2012).

3 Data

To reconstruct the global distribution of CO_2 from UT to the stratosphere, we need to assign the backward trajectories with the free tropospheric CO_2 field. This is achieved by using two
25 different types of CO_2 data: ground stations (Worden et al., 2015) and CarbonTracker (Peters et al., 2007). We first focus on the free tropospheric CO_2 field.



3.1 Construction of the free tropospheric CO₂ field

Two different observation-based data sets are used to assign CO₂ to the backward trajectories in the Lagrangian model depending on the time period considered.

During the 1989–1999 time period, data from ground stations of the World Data Centre for Greenhouse Gases (WDCGG) are used to assign the integrated air particles. The WDCGG is an international data center participating in Global Atmosphere Watch. It provides extensive data from ground stations and aircraft measurements across the Earth that are non-homogeneously distributed. To model the CO₂ emissions, the monthly CO₂ data from ground stations (e.g. Mauna Loa, South Pole and others) located at different latitudes have been used to overcome the daily fluctuations of the CO₂ in the atmospheric boundary layer. The criterion to select the ground stations is that the location is assured to be high enough to neglect the daily variability due to the contribution of localized sources at ground level. The CO₂ data are averaged from pole to pole in latitude increments of 30° and over all longitudes to represent the global, free tropospheric CO₂ field. To better model the latitude dependence of the seasonal cycle and to overcome discontinuities, the averaged CO₂ data obtained are then interpolated linearly along the latitude. This is our baseline for injecting CO₂ values to constrain the backward trajectories from the model during the 1989–1999 time period.

During the remaining time period 2000–2010, we use the most recent CO₂ mole fractions released in a longitude × latitude grid (3° × 2°) from the coupled CTM TM5 and the data assimilation system, CarbonTracker, to assign the backward trajectories. Similar to the 1989–1999 time period, we consider these CO₂ from CarbonTracker only at 5 km level (500 hPa), which is above the atmospheric boundary layer. The CarbonTracker system assimilates different types of CO₂ measurements, which come from ocean surface fluxes, atmospheric stations, biosphere activity monitoring, fire burning and fossil fuel burning emissions inventoried in many regions. These data are important to achieve a complete and realistic diagnostic of the atmospheric CO₂ and fluxes (CarbonTracker-2013B, www.esrl.noaa.gov/gmd/ccgg/carbontracker/). This last archive of CO₂ is more accurate than the previous because of the recent correction of TM5 in reproducing a realistic convective flux due to a fault in one of the vertical mixing



parametrisations of the model.

3.2 *In situ* aircraft and balloon measurements

The SAGE III Ozone Loss and Validation Experiment (SOLVE) was a measurement campaign designed to examine the processes controlling ozone levels at mid- to high latitudes. Measurements were made in the Arctic high-latitude region in winter using the NASA DC-8 and ER-2 aircrafts, as well as balloon platforms and ground-based instruments. The mission also acquired correlative data needed to validate the Stratospheric Aerosol and Gas Experiment (SAGE) III satellite measurements that is used to quantitatively assess high-latitude ozone loss.

The SOLVE campaign sought to establish a comprehensive data set of UTLS trace gases and meteorological data in the northern polar regions, including latitudinal gradients across the polar vortex. The campaign took place during the period October 1999 to March 2000. CO₂, CH₄ and N₂O were measured by several instruments and used to calculate a composite AoA (Andrews et al., 2001b).

In the UTLS, there are strong horizontal and vertical gradients. These gradients may occur on a small scale and show a high temporal and spatial variability. In this study, we were interested in airborne measurements to characterize the stratospheric variability and mixing process as well as to validate our model. The aircraft atmospheric measurements have a huge advantage for the spatial resolution and offer the possibility to capture with high precision small scale variations. Aircraft observations have a vertical resolution of a few meters and a horizontal resolution of a few hundred meters resulting from the high sampling frequency of these instruments (0.5-2 Hz). Test and transit flights, made at mid-latitudes, were used to illustrate the comparison of the calculated CO₂.

In situ balloon-based CO₂ profile measurements are used as basis for comparisons with the reconstructed CO₂ from the Lagrangian transport model. The data sets are high-quality observations with sufficient altitude coverage and are from measurements of whole air samples collected cryogenically from balloons or from *in situ* measurements on-board a balloon gondola (Engel et al., 2009; Ray et al., 2014). Four balloon flights covering the time period from 2001 to 2005 and the latitudes range from 34° to 44°N with a vertical resolution of a few me-



ters are used in this study. Only these four balloon flights contained the CO₂ profiles that were measured at Ft. Sumner, New Mexico, USA (34.5 °N) on 17 September 2004, Sanriku, Japan (39.33 °N) on 30 May 2001, Aire sur L'Adour, France (43.5 °N and 44 °N) on 24 September 2002 and on 9 October 2001, respectively. Note that most profile observations are from the
5 May to October period, when stratospheric variability in the northern hemisphere is expected to be lower than during the winter period. These measurements of very long-lived trace gases, which increase with time in the troposphere and have neither atmospheric sinks nor sources of significance in the relevant parts of the atmosphere, have been used to derived the mean AoA (Andrews et al., 2001a; Engel et al., 2009) but here we focus on CO₂.

10 **4 Initialisation of air particles**

In order to calculate the global CO₂ distribution, air particles are initialized from the UT to the stratosphere their backward integrations. This initialisation is described below.

4.1 CO₂ global initialisation

The global initialisation aims to obtain a zonal mean distribution of CO₂ in order to investigate
15 the mechanism of the BDC over the whole UT/S. To perform this study so, we assign these air particles globally integrated in the Sect. 2 with the reconstructed free tropospheric CO₂ field in Sect. 3.1 over the UT and the whole stratosphere.

In the model the assignation of the reconstructed free tropospheric CO₂ field (Sect. 3.1) is performed according to latitudinal and longitudinal position of the air particle for a given time.
20 Each trajectory is integrated backward to the troposphere and at that point we assign the free tropospheric CO₂ to it at that time based on wherever the trajectory reaches the tropospheric boundary condition. It is assumed that the vertical mixing is fast in the troposphere, which is verified in the inner tropical region, where are the sources of the stratospheric air (Brewer, 1949). As the air particle moves upward across the boundary level, it retains its last value of
25 CO₂ inherited from the boundary condition. The CO₂ value of the air particle is then advected



into the stratosphere by the different branches of stratospheric circulation.

The monthly mean CO₂ for a given box in latitude and altitude (typically 2° × model level spacing) and for a given month is calculated as the average in longitude circle over all particles falling within this box (Fig. 1). This calculation uses the same approach as Sect. 2.3 in Diallo et al. (2012). Owing to the quasi-uniform spread of the discrete trajectories at the initialisation stage, the average is made over 180 particles at the equator and over 67 particles at 68° N or S. Latitudes closer to the pole are grouped into enlarged latitude bins (69°–73°, 73°–77°, 77°–81°, 81°–90°) to avoid large fluctuations due to the reduced number of particles. Further averaging over time is performed to improve statistics and to reduce noise. These averaging procedures are a simple way to account for mixing in the stratosphere and gather within each box a distribution of particles with different histories.

As observed by Scheele et al. (2005), the number of backward trajectories launched at a given date and remaining within the stratosphere after some delay age (e.g. time residence), τ , decreases exponentially with τ . Figure 1 in Diallo et al. (2012) shows that this law is indeed very well satisfied for $\tau > 3\text{yr}$ with an exponential decrement $b = 0.2038\text{yr}^{-1}$ for the mean decay in ERA-Interim and that the standard deviation from the mean (when each month is considered separately) decays at the same rate. After 10 years of backward motion, 88 % of the particles launched within the stratosphere have met the tropopause. We follow Scheele et al. (2005) in using this property to correct the estimated CO₂ for the truncation of trajectory lengths at 10 years. If we define $G(\tau, t)$ as the cumulative probability density of the age τ , the monthly mean CO₂ is

$$\overline{\text{CO}_2}(t) = \int_0^\infty \text{CO}_2(t-\tau) \cdot G(t, \tau) d\tau. \quad (1)$$

The truncated version of this integral, up to $t_f = 10\text{yr}$, can be calculated explicitly from the backward trajectories. Assuming that $G(t, \tau) = G(t, t_f) \cdot \exp(-b(\tau - t_f))$ for $t > t_f$ with $\text{CO}_2(\tau) = p_0 + p_1 \cdot \tau + b_0 \cdot \cos(2\pi(\tau - \varphi))$ obtained by fitting the Mauna Loa CO₂ data, the monthly mean CO₂ can be estimated as



$$\overline{\text{CO}_2}(t) = \int_0^{t_f} \text{CO}_2(t - \tau) \cdot G(t, \tau) d\tau + \frac{G(t, t_f)}{b} \left(p_0 + p_1 \cdot \left(t - t_f - \frac{1}{b} \right) \right) + \text{Corr}(t), \quad (2)$$

with

$$\text{Corr}(t) = \frac{b_0 \cdot G(t, t_f)}{b^2 + 4\pi^2} \left[b \cdot \cos \left(2\pi(t - t_f - \varphi) \right) + 2\pi \cdot \sin \left(2\pi(t - t_f - \varphi) \right) \right]. \quad (3)$$

The obtained zonal mean distribution of CO_2 is further discussed below but currently we focus on the reconstructed CO_2 for the SOLVE campaign in order to test the ability of the Lagrangian model to reproduce the aircraft measurements.

4.2 Validations of the technique

- 5 The *in situ* measurement location initializations during SOLVE and balloon campaigns are used for validation of the global initialisation of air particles.

4.2.1 SOLVE flight track initialisation

The ER-2 flight initialisation is made by using the airborne measurements during the SOLVE campaign. The particles are initialized along the flight trajectory with a frequency identical to that of the tracer measurements (0.25 Hz). For this calculation, a set of 200 particles are
10 initialised at the same position as those measured during the flight in order to take into account the diffusive processes e.g. each air parcel is actually a mixture of particles from various origins. These particles are released every 4 s and integrated backward over 6 months with a diffusivity parameter κ equal to $0.1 \text{ m}^2 \text{ s}^{-1}$ that represents the turbulent diffusion D (Eq: 6) due to small-
15 scale motion missing in the ECMWF winds (Legras et al., 2005). This procedure is chosen because it is consistent with the underlying physics and also because the applied diffusion can be estimated from the comparison of small-scale observed tracer fluctuations and reconstructions (Legras et al., 2005; Pisso and Legras, 2008). After a few days, the notion of isolated air parcel in the atmosphere loses its consistency. This model is a discretised approximation of the Green
20 function obtained by integrating the adjoint advection-diffusion equation backward in time.



The dispersion of particles is done by adding a random vertical noise into the calculation of each trajectory and at each time step representing the turbulent diffusion κ due to small scale movements not taken into account in wind fields (Legras et al., 2003). The displacement X of air particles over a small time interval δt , is described by

$$\delta \mathbf{X} = v(\mathbf{X}, t) \cdot \delta t + \delta \eta(t) \cdot \mathbf{k} \quad (4)$$

5 where the white noise process for the mixing is $\delta \eta(t) \equiv w \delta t$ and \mathbf{k} is the unit vector. The process is without memory (i.e it is δ -correlated), and with a zero mean. If the limit $\delta t \rightarrow 0$ and after statistical average over a large number of particles, this is equivalent to adding a diffusion to transport such the concentration tracer, C , is no longer conserved. Then advection-diffusion equation is

$$\frac{\partial C}{\partial t} + v \cdot \nabla C = \kappa \frac{\partial^2 C}{\partial \theta^2}, \quad (5)$$

10 with

$$\kappa = \frac{1}{2} \langle w^2 \rangle \delta t \quad (6)$$

w is derived from a white noise normalized by the value of the diffusion coefficient κ defined by the user and δt is the time step. In order to ensure that vertical velocities are bounded, we use a white noise based on a random variable r that is uniformly distributed with zero mean and unite variance. Applying 6, the random process is then $\delta \eta = r \sqrt{2\kappa \delta t}$, where $\delta \eta$ is the vertical displacement with a new drawing of r at each time step and for each particles. A corresponding displacement in θ is applied for diabatic runs using the adiabatic conversion function

$$\frac{\delta \theta}{\delta \eta} = \left(\frac{p_o}{p} \right)^\kappa \frac{g}{C_p}. \quad (7)$$

After the backward integration of few months, then the air particles of the diffusive run are fixed by using the ages calculated from the global initialisation.



4.2.2 Balloon flight initialisation

The balloon flight initialisation is made by using the *in situ* measurements campaign described in Engel et al. (2009). The particles are initialized along the balloon flight trajectory with a frequency higher than the tracer measurements. A set of 5000 particles are initialised over 200
5 vertical levels ranging from 500 hPa to 1 hPa at the same latitude-longitude position as those measured by the balloon flights. These particles are released as the balloon moves upward and integrated backward over 6 months with a diffusivity parameter κ equal to $0.1 \text{ m}^2 \cdot \text{s}^{-1}$ (Legras et al., 2005). After a few days, because of the consistency lost due to the notion of non-isolated air parcel in the atmosphere, we apply a same technique for the dispersion of particles. The
10 mean CO_2 is obtained by constraining these backward trajectories with those calculated by the global initialisation.

5 Reconstructed CO_2

In order to determine how tracer distribution is controlled by transport and small scale of mixing into the extra-tropical LMS, we investigate how Lagrangian diffusive reconstructions (Legras et al., 2005; James and Legras, 2009) are able to reproduce the observed CO_2 (Andrews et al.,
15 2001b; Daube et al., 2002; Park et al., 2007a; Engel et al., 2009; Ray et al., 2014).

5.1 SOLVE campaign

Here we reconstruct the CO_2 measured from the ER-2 flights in the polar regions during the SOLVE campaign using backward trajectories. The reconstructed CO_2 is obtained by averaging
20 the CO_2 values at the locations reached by the air particles integrated in Sect. 4.2.1 after the end of the backward integration. These reconstructions exhibit a good agreement with the observations (red) from Daube et al. (2002). In all cases, the measurements fall within the 95% confidence interval of the reconstruction and in many instances reproduce the small scale variations as well. The large peaks seen, e.g., on 20000202, 20000226, 20000131 are due to
25 dives and the discontinuities on 20000203 and 20000114 are also due to fast altitude changes.



However, on 20000127 and 20000311 the sharp discontinuities of CO₂ are due to the repeated crossing of the vortex edge and peeled off filaments outside the edge (Konopka et al., 2003; Legras et al., 2005). In some cases, like 20000203, the confidence interval gets larger and the agreements is lower because the flight stayed within a region of high sensitivity to trajectory
5 fluctuations (near an hyperbolic point, see Koh and Legras (2002)) due to a vortex splitting event. On 20000307, the flight occurred in the ageing vortex core. The too low prediction of TRACZILLA might be due to the large contribution of the corrective step (see section 4.1) in this instance.

The overall conclusion of this section is that reconstructed CO₂ by TRACZILLA, based on
10 advection with resolved winds and a simple parameterisation of mixing by diffusion, explains very well the measurements made by the ER-2 aircraft during the Arctic SOLVE campaign.

5.2 Balloon vertical profiles

It is also interesting to perform a detailed comparison with balloon soundings which span a larger vertical range than the aircrafts. Such a comparison of the vertical profiles of the re-
15 constructed mean CO₂ by TRACZILLA with those derived from observations of four middle stratospheric balloon flights (Engel et al., 2009; Ray et al., 2014) is shown in Fig. 3.

For three of the cases, most of the measurements fall within the 95% confidence interval of the reconstructed profiles and the local maxima at 23 km and 18 km on 20020924 and 20050901 are well reproduced. The reconstructed profile on 20011009 is significantly different from the
20 observed profile. The balloon was launched from Aire sur l'Adour (France) while the area was crossed by a cold front associated with strong tracer gradient in the upper atmosphere (see the insert in Fig. 3). In such situations, the errors of the reanalysis which are not accounted in our statistical test might be large enough to explain the shift.

The reconstructed vertical profiles of the mean CO₂ is in very good agreement with all the
25 *in situ* CO₂ measurements at all altitudes, even in the small scale variations occurring in the 15–25 km bin except in the profile at 44 °N, which exhibits a spread behavior (Fig. 3). The mean *in situ* CO₂ from observations is much more spread in the high latitude profiles (44 °N) above 15 km. There is not a clear explanation about these observed fluctuations on the *in situ*



CO₂ profile.

Figure 3 also illustrate the increase of the stratospheric CO₂ abundance from 2001 (upper left) to 2005 (lower right). Again, the reconstructions show the ability of TRACZILLA to capture the features in the vertical propagation of the tracer variations even in the small scales.

5 5.3 Temporal series

To obtain additional accurate details about the upward propagation of the tropospheric CO₂ seasonal cycle into the LMS, we compare the temporal evolution of the monthly mean CO₂ from the global initialisation (Sect. 4.1) calculated by TRACZILLA with those derived from observations over several months. We choose the latitudes ranges 10°S–20°N and 50–60°N to validate the tropospheric and stratospheric boundary conditions for CO₂ time series from TRACZILLA.

The top panel of Fig. 4 shows the comparison of the time series of modelled monthly mean CO₂ with those from CONTRAIL (Sawa et al., 2008, 2012) in the 10°S–20°N at 8–9 km altitude bins over the same time period August 2006 to January 2010. The comparisons are generally in good agreement with observations, which shows the ability of the model to capture the tropospheric CO₂ seasonal variation and the validation of tropospheric boundary condition.

The mid panel of Fig. 4 compares the modelled monthly mean CO₂ time series in a layer at 16–17 km and between 10 S and 20 N just below the tropical tropopause with the average of ground-based CO₂ data from Mauna Loa (19°N) and American Samoa (14°S) delayed by 15 days. We find, consistently with Boering et al. (1996) and Andrews et al. (1999, 2001a,b), that the amplitude of the two signals is the same but our delay is shorter than the two months found in previous studies. We recover a two-month delay at higher altitude in the layer 18–19 km (not shown). The origin of this discrepancy is unclear but is perhaps due to the fact that previous studies merge measurements in the deep tropics and the subtropics.

The bottom panel of Fig. 4 shows the modelled monthly mean CO₂ in the latitude bin 50–60°N at different altitudes ranging from 7–13 km over the same time period November 2005 to January 2010. These curves are compared with CONTRAIL measurements in the same latitude band (Sawa et al., 2008). The modelled and measured CO₂ differ generally by less than 1 ppmv



except a few isolated months like March 2006 and March 2009. Notice also the large deviation of the 12-13 km CONTRAIL measurement in April 2007. There is a shift of the order of 4–6 months of the mean CO₂ seasonal cycle above 11–12 km with respect from the tropospheric signal. This is due to the delay induced by the shallow branch of the BDC also found by Bönisch et al. (2009) and Sawa et al. (2008). The large discrepancies concentrated during the spring season suggest that large gradients of CO₂ span the measurement are in this period, as it will be confirmed shortly.

6 Global distribution of the zonal mean CO₂

The zonal mean distribution of CO₂ illustrates the main features of the BDC, such as mixing and transport variabilities through temporal and spatial evolution. Figure 5 shows the typical seasonal variation of the monthly mean CO₂ in latitude-altitude cross sections calculated by the Lagrangian transport model for 2010.

6.1 Upper-troposphere and Lowermost stratosphere

The zonal mean distribution of CO₂ in the free atmosphere, especially above 5 km, is driven by the large-scale transport processes. Fast quasi-isentropic mixing is combined with upwelling in the tropics and downwelling in the extra-tropical lowermost stratosphere. Figure 5 shows that, in the northern hemisphere, the tropospheric monthly mean CO₂ is dominated by a strong seasonal cycle in the UT reflecting the activity (breathing of photosynthesis and respiration). CO₂ concentration grow during fall and winter to reach a maximum in April-May followed by a rapid decay due to the spring biospheric bloom and reach a minimum in July-August. The cycle is much weaker in the Southern hemisphere and influenced by the transport from the northern hemisphere. The combined effect of fast isentropic mixing (Haynes and Shuckburgh, 2000a,b) and convection (Sawa et al., 2008) propagates the cycle towards the tropics creating both horizontal and vertical gradients (Nakamura et al., 1991; Bönisch et al., 2009; Sawa et al., 2012). It is visible in Fig. 5 that during the northern hemisphere winter the concentration tends



to follow the isentropes in the extra-tropics. The barrier effect of the subtropical jet (Miyazaki et al., 2009) generates a strong meridional gradient near 30 °N, which is maximum near 350 K. Once it has reached the tropic, CO₂ is then transported upward by tropical convection and propagated to the stratosphere through the BDC. Throughout the spring and summer, while the tropospheric CO₂ is pumped out by the biosphere, a layer of high CO₂ extends from the tropics to the northern mid-latitudes in the lower stratosphere due to the lower branch of the BDC (Bönisch et al., 2008). This transport is favored by the Asian monsoon anticyclone, which traps young air lofted from the surface and induces a flux to the extra-tropical stratosphere on its West side as it is eroded across the jet (Dethof et al., 2000; Bannister et al., 2004; Park et al., 2007b, 2008, 2009, 2010; Randel et al., 2010). Due to the time delay of this transport, the maximum concentration of CO₂ in the northern lower stratosphere lags by 4 to 6 months that at the surface and is reached basically when the surface concentration is at its minimum. The result is an inverted vertical profile, which is a maximum in July and persists over the summer. A qualitative comparison between the reconstructed CO₂ in Fig. 5 and observation from Sawa et al. (2008) (see their figure 7) exhibits a good agreement in the cycle of the tropospheric and lower stratospheric CO₂ and in particular in the cycle of the inversion. There are, however, differences in the location and intensity of the meridional gradient, which might be due to the specific sampling of Sawa et al. (2008) that gives a strong weight to the most intense region of the Pacific jet stream.

6.2 Middle and upper Stratosphere

As the tropospheric seasonal cycle is transported into the middle and upper stratosphere through the *tropical pipe* and mid-latitude tropopause crossing, its amplitude decreases upward because of the combined effect of the upwelling branch of the BDC and mixing processes. The deep branch of the BDC is much slower than the shallow branch and old air with low CO₂ concentrates in the middle and upper stratosphere. The tropical pipe isolate young air with high CO₂, an effect, which is maximum during northern hemisphere winter in agreement with age of air calculations (Li et al., 2012; Diallo et al., 2012). The horizontal mixing homogenizes CO₂ in the mid and high latitudes. Because of this prior mixing the winter containment within the po-



lar vortex does generates only a weak polar minimum (and no localized gradient as we average over latitude circle and not following the CO₂ contours).

6.3 Spring-Summer vertical profiles

In this section, monthly averaged CO₂ profiles are investigated to understand the changes in the CO₂ vertical structure within the UT/S (Fig. 6).

On the left panel, the spring-summer reconstructed vertical profiles of the CO₂ compared with those from CONTRAIL aircraft measurements for the year 2007 at 50–60 °N show a good tropospheric agreement and an inversion of the CO₂ vertical gradient during August in the LMS. The monthly mean CO₂ vertical profiles, calculated by backward trajectories, exhibits a complex vertical structure with gradient layers interspelled with no gradient layers.

The annual structure of the profile is made apparent in the right panel where we show averaged monthly profiles over the period 2000-2010 after removal of the mean CO₂ trend at each level. Starting from January, the increase of CO₂ in the troposphere penetrates upward in the stratosphere over the limited vertical range of the Extra-tropical Transition Layer (Hegglin et al., 2010; Gettelman et al., 2011) (ExTL), that is over 2 to 3 km above the tropopause as visible on the March profile. Between March and May, another processus occurs, which inject young air rich in CO₂ above 13 km. This can only be due to a tropical intrusion favored by the weakening of the tropical barrier at the end of the winter. The profile suggests that the intrusion is deep from 13 to about 23 km, that the well-mixed layer between 13 and 16 km is inherited from the well-mixed tropical tropospheric profile at such altitudes and that the mixing layer between 16 and 23 km is also inherited from the tropical lower stratosphere vertical gradient. The mixing layer persists with the same slope during the whole summer and the bottom of the intrusion corresponds to the maximum of CO₂ when the inversion is at its maximum. During fall, when the subtropical barrier is re-established, the gradient weakens, the residual well-mixed layer disappears and the profile returns to the fairly uniform shape of January.



7 Conclusions

We have reconstructed a zonal mean distribution of CO₂ at global scale ranging from the upper-troposphere to stratosphere using Lagrangian trajectories guided by reanalysed winds and heating rates from the ERA-Interim. This study is based on 22 years of data and provides a monthly mean CO₂ over the last 11 years (2000–2010). We have also performed direct reconstruction of different *in situ* campaigns, such as SOLVE, stratospheric balloons campaigns and CONTRAIL, that has been compared with these observations to validate the reconstructed CO₂.

Our reconstructed CO₂ for the ER-2 aircraft flight tracks as well as for the vertical balloon profiles and time series using TRACZILLA show remarkable agreement even in the small scale variations with *in situ* observations from SOLVE, stratospheric balloons and CONTRAIL campaigns, respectively. This demonstrates that this Lagrangian model is able to reproduce most of the observed transport and mixing variability along the aircraft flight track, to capture the features in the vertical propagation of the tracer variations and to represent well the tropospheric and stratospheric boundary conditions. This reconstruction suggests that the distribution of long-lived tracers, such as CO₂, can be explained by the properties of transport as resolved by meteorological analysis and a simple representation of sub-grid scale effects as a diffusion.

The zonal mean distribution of CO₂ accurately reproduces the main feature of the stratospheric circulation variability through the upward and meridional propagation of the seasonal cycle extending from the upper-troposphere to the stratosphere.

In the northern hemisphere troposphere, the monthly mean CO₂ is dominated by biospheric activity and displays a strong seasonal cycle, which is vertically and horizontally propagated to the tropopause and above in the ExTL on the one hand and to the tropics on the other hand. In the regions of high horizontal mixed, as the mid-latitudes the CO₂ tends to uniformise over isentropic surfaces. Meridional gradients are localized over transport barrier such as the subtropical jet during winter.

Transport of CO₂ to the northern extra-tropical stratosphere above the ExTL is to a large extent due to the export of tropical air. The long circuit of CO₂ from the extra-tropics to the tropics in the troposphere and then back to the extra-tropics in the stratosphere induces a time lag



of 4–6 months such that the tropospheric and stratospheric variability are almost in opposition at mid-altitudes. The result is the production of an inverted CO₂ profile during summer.

In the deep stratosphere, we have found that as the tropospheric seasonal cycle is transported into the stratosphere through the *tropical pipe* and mid-latitude tropopause crossing, its amplitude is smoothed out upward the stratosphere because of the combined effect of the upwelling branch of the BDC and quasi-horizontal mixing. A more confined *tropical pipe* is found in the tropical band during the winter and spring than during summer and autumn.

Finally, the zonal mean distribution of CO₂ is a unique data set of a critical trace gas, that has a variety of uses. We have compiled this new relevant database of CO₂ global distribution from 2000–2010 for use to validate the representation of upper-tropospheric and stratospheric tracer distributions in CTMs, in CCMs and to test the representativeness of aircraft Measurements. The data set includes monthly-averaged two-dimensional fields gridded on the model's 77 latitudes and 36 vertical levels varying from 90° S to 90° N and from 5 km to 42 km respectively.

Acknowledgements. We particularly thank Y. Sawa, H. Matsueda and T. Machida for providing CO₂ measurements from CONTRAIL, the ECWMF for providing reanalysis data, WD-CGG for providing the ground station CO₂ data from 1989–1999, CarbonTracker team for providing the CO₂ data from 2000–2010. We thank Harald Bonisch for comments and helpful discussions. We acknowledge support from the EU 7th framework Program under grant 603557 (StratoClim). M. Diallo was mainly supported by a postdoctoral grant from the ExCirEs Project (CGL2011-24826) funded by the Government of Spain. Further thanks to the CICLAD cluster at the Institut Pierre Simon Laplace in Paris on which most parts of this work had been carried out. The TRACZILLA model CO₂ data set may be requested from the corresponding author (mdiallo@lmd.ens.fr).



References

- Abalos, M., Legras, B., Ploeger, F., and Randel, W. J.: Evaluating the advective Brewer-Dobson circulation in three reanalyses for the period 1979–2012, *J. Geophys. Res. Atmos.*, 120, 7534–7554, doi:10.1002/2015JD023182, 2015.
- 5 Andrews, A. E., Boering, K. A., Daube, B. C., Wofsy, S. C., Hints, E. J., Weinstock, E. M., and Bui, T. P.: Mean age of stratospheric air derived from in situ observations of CO₂, CH₄ and N₂O, *J. Geophys. Res.*, 106, 32 295–32 314, doi:10.1029/2001JD000465, 1999.
- Andrews, A. E., Boering, K. A., Wofsy, S. C., Daube, B. C., Jones, D. B., Alex, S., Loewenstein, M., Podolske, J. R., and Strahan, S. E.: Empirical age spectra for the lower tropical stratosphere from
10 in situ observations of CO₂: Quantitative evidence for a sub-tropical barrier to horizontal transport, *J. Geophys. Res.*, 106, 32,295–32,314, doi:10.1029/2001JD000465, 2001a.
- Andrews, A. E., Boering, K. A., Daube, B. C., Wofsy, S. C., Loewenstein, M., Jost, H., Podolske, J. R., Webster, C. R., Herman, R. L., C., S. D., Flesch, G. J., Moyer, E. J., Elkins, J. W., Dutton, G. S., Hurst, D. F., Moore, F. L., Ray, E. A., Romashkin, P. A., and Strahan, S. E.: Mean age of stratospheric air
15 derived from in situ observations of CO₂: Implications for stratospheric transport, *J. Geophys. Res.*, 104, 26 581–26 596, doi:doi:10.1029/1999JD900150, 2001b.
- Andrews, D. G., Holton, J. R., and Leovy, C. B.: Middle Atmosphere Dynamics, vol. 40 of *International Geophysics Series*, Academic Press, San Diego, USA, 1987.
- Bannister, R. N., O’Neil, A., Gregory, A. R., and Nissen, K. M.: The role of the south-east Asian
20 monsoon and other seasonal features in creating the ‘tape-recorder’ signal in the Unified Model, *Q. J. R. Meteorol. Soc.*, 130, 1531–1554, doi:10.1256/qj.03.106, 2004.
- Bernath, P. F., McElroy, C. T., Abrams, M. C., Boone, C. D., Butler, M., Camy-Peyret, C., Carleer, M., Clerbaux, C., Coheur, P.-F., Colin, R., DeCola, P., DeMaziere, M., Drummond, J. R., Dufour, D., Evans, W. F. J., Fast, H., Fussen, D., Gilbert, K., Jennings, D. E., Llewellyn, E. J., Lowe, R. P.,
25 Mahieu, E., McConnell, J. C., McHugh, M., and R. Michaud, S. D. M., Midwinter, C., Nassar, R., Nichitui, F., Nowlan, C., Rinsland, C. P., Rochon, Y. J., Rowlands, N., Semeniuk, K., Simon, P., Skelton, R., Sloan, J. J., Soucy, M.-A., Strong, K., Tremblay, P., Turnbull, D., Walker, K. A., Walkty, I., Wardle, D. A., Wehrle, V., Zander, R., and Zou, J.: Atmospheric Chemistry Experiment (ACE): Mission overview, 32, doi:doi:10.1029/2005GL022386, 2005.
- 30 Boering, K. A., Wofsy, S. C., Daube, B. C., Schneider, H. R., Loewenstein, M., Podolske, J. R., and Conway, T. J.: Stratospheric mean ages and transport rates from observations of carbon dioxide and nitrous oxide, *Science*, 274, 1340–1343, doi:10.1126/science.274.5291.1340, 1996.



- Bönisch, H. B., Hoor, P., Gurk, C., Feng, W., Chipperfield, M., Engel, A., and Bregman, B.: Model evaluation of CO₂ and SF₆ in the extratropical UT/LS region, *J. Geophys. Res.*, 113, D06 101, doi:10.1029/2007JD008829, 2008.
- 5 Bönisch, H. B., Engel, A., Curtius, H., Birner, T., and Hoor, P.: Quantifying transport into the lowermost stratosphere using simultaneous in-situ measurements of SF₆ and CO₂, *Atmos. Chem. Phys.*, 9, 5905–5919, doi:10.5194/acp-9-5905-2009, 2009.
- Bönisch, H. B., Engel, A., Birner, T., Hoor, P., Tarasick, D. W., and Ray, E. A.: On the structural changes in the Brewer-Dobson circulation after 2000, *Atmos. Chem. Phys.*, 11, 3937–3948, doi:10.5194/acp-11-3937-2011, 2011.
- 10 Boucher, O., Friedlingstein, P., Collins, B., and Keith P Shine, K. P.: The indirect global warming potential and global temperature change potential due to methane oxidation, *Environ. Res. Lett.*, 4, doi:10.1088/1748-9326/4/4/044007, 2009.
- Bowman, M., Rozanov, V. V., and Burrows, J. P.: A near-infrared optimized DOAS method for the fast global retrieval of atmospheric CH₄, CO, CO₂, H₂O, and N₂O total column amounts from SCIAMACHY Envisat-1 nadir radiances, *J. Geophys. Res.*, 105, 15,231–15,245, doi:10.1029/2000JD900191, 2000.
- 15 Brewer, A.: Evidence for a world circulation provided by the measurements of helium and water vapour distribution in the stratosphere, *Q. J. R. Meteorol. Soc.*, 75, 351–363, 1949.
- Butchart, N., Cionni, I., Eyring, V., Shepherd, T. G., Waugh, D. W., Akiyoshi, H., Austin, J., Br¹/₄hl, C., Chipperfield, M. P., Cordero, E., Dameris, M., Deckert, R., Dhomse, S., Frith, S. M., Garcia, R. R., Gettelman, A., Giorgetta, M. A., Kinnison, D. E., Li, F., Mancini, E., McLandress, C., Pawson, S., Pitari, G., Plummer, D. A., Rozanov, E., Sassi, F., Scinocca, J. F., Shibata, K., Steil, B., and Tian, W.: Chemistry-Climate Model simulations of twenty-first century stratospheric climate and circulation changes, *J. Climate*, 23, 5349–5374, doi:10.1175/2010JCLI3404.1, <http://dx.doi.org/10.1175/2010JCLI3404.1>, 2010.
- 25 Chedin, A., Hollingsworth, A., Scott, N. A., Serrar, S., Crevoisier, C., and Armante, R.: Annual and seasonal variations of atmospheric CO₂, N₂O and CO concentrations retrieved from NOAA/TOVS satellite observations, *Geophys. Res. Lett.*, 29, 1269, doi:10.1029/2001GL014082, 2002a.
- Chedin, A., Serrar, S., Armante, R., Scott, N. A., and Hollingsworth, A.: Signatures of Annual and Seasonal Variations of CO₂ and Other Greenhouse Gases from Comparisons between NOAA TOVS Observations and Radiation Model Simulations., *J. Climate*, 15, 95–116, doi:10.1175/1520-0442(2002)015<0095:SOAASV>2.0.CO;2, 2002b.
- 30 Chedin, A., Saunders, R., Hollingsworth, A., Scott, N., Matricardi, M., Etcheto, J., Clerbaux, C.,



- Armante, R., and Crevoisier, C.: The feasibility of monitoring CO₂ from high-resolution infrared sounders, *J. Geophys. Res.*, 108, 4064, doi:10.1029/2001JD001443, 2003a.
- Chedin, A., Serrar, S., Scott, N. A., Crevoisier, C., and Armante, R.: First global measurement of midtropospheric CO₂ from NOAA polar satellites: Tropical zone, *J. Geophys. Res.*, 108, 4581, doi: 10.1029/2003JD003439, 2003b.
- 5 Daube, B. C. J., Boering, K. A., Andrews, A. E., and Wofsy, S. C.: A High-Precision Fast-Response Airborne CO₂ Analyzer for In Situ Sampling from the Surface to the Middle Stratosphere, *J. Atmos Oceanic Technol.*, 19, 1532–1543, doi:10.1175/1520-0426(2002)019<1532:AHPFRA>2.0.CO;2, 2002.
- 10 Dethof, A., O'Neill, A., and Slingo, J.: Quantification of the isentropic mass transport across the dynamical tropopause, *J. Geophys. Res.*, 105, 12 279–12 293, doi:10.1029/2000JD900127, 2000.
- Diallo, M., Legras, B., and Chédin, A.: Age of stratospheric air in the ERA-Interim, *Atmos. Chem. Phys.*, 12, 12 133–12 154, doi:10.5194/acp-12-12133-2012, 2012.
- 15 Eluszkiewicz, J., Hemler, R. S., Mahlman, J. D., Bruhwiler, L., and Takacs, L. L.: Sensitivity of Age-of-Air Calculations to the Choice of Advection Scheme, *J. Atmos. Sci.*, 57, 3185–3201, doi:10.1175/1520-0469(2000)057<3185:SOAOAC>2.0.CO;2, 2000.
- Engel, A., Bönisch, H., Brunner, D., Fischer, H., Franke, H., Günther, G., Gurk, C., Hegglin, M., Hoor, P., Königstedt, R., Krebsbach, M., Maser, R., Parchatka, U., Peter, T., Schell, D., Schiller, C., Schmidt, U., Spelten, N., Szabo, T., Weers, U., Wernli, H., Wetter, T., and Wirth, V.: Highly resolved observations of trace gases in the lowermost stratosphere and upper troposphere from the Spurt project: an overview, *Atmos. Chem. Phys.*, 6, 283–301, doi:10.5194/acp-6-283-2006, 2006.
- 20 Engel, A., Möbius, T., Bönisch, H., Schmidt, U., Heinz, R., Levin, I., Atlas, E., Aoki, S., Nakazawa, T., Sugawara, S., Moore, F., Hurst, D., Elkins, J., Schaufli, S., Andrews, A., and Boering, K.: Age of stratospheric air unchanged within uncertainties over the past 30 years, *Nature Geoscience*, 2, 28–31, doi:10.1038/ngeo388, 2009.
- 25 Forster, P. M., Ramaswamy, V., Artaxo, P., Berntsen, T., Betts, R., Fahey, D. W., Haywood, J., Lean, J., Lowe, D. C., Myhre, G., Nganga, J., Prinn, R., Raga, G., Schulz, M., and Van Dorland, R.: Changes in atmospheric constituents and in radiative forcing Climate Change 2007: The Physical Science Basis. Contribution of Working Group I to the Fourth Assessment Report of the Intergovernmental Panel on Climate Change [S. Solomon, D. Qin, M. Manning, Z. Chen, M. Marquis, K.B. Averyt, M. Tignor and H.L. Miller (eds.)], Cambridge University Press, Cambridge, United Kingdom and New York, NY, USA, pp. 129–234, 2007.
- 30 Forster, P. M. D. F. and Shine, K. P.: Radiative forcing and temperature trends from stratospheric ozone



- changes, *Geophys. Res. Lett.*, 102, 10 841–10 855, doi:10.1029/96JD03510, 1997.
- Foucher, P. Y., Chedin, A., Armante, R., Boone, C., Crevoisier, C., and Bernath, P.: Technical Note: Feasibility of CO₂ profile retrieval from limb viewing solar occultation made by the ACE-FTS instrument, *Atmos. Chem. Phys.*, 9, 2873–2890, doi:10.5194/acp-9-2873-2009, 2009.
- 5 Foucher, P. Y., Chedin, A., Armante, R., Boone, C., Crevoisier, C., and Bernath, P.: Carbon dioxide atmospheric vertical profiles retrieved from space observation using ACE-FTS solar occultation instrument, *Atmos. Chem. Phys.*, 11, 2455–2470, doi:10.5194/acp-11-2455-2011, 2011.
- Frankenberg, C., Pollock, R., Lee, R. A. M., Rosenberg, R., Blavier, J.-F., Crisp, D., O’Dell, C. W., Osterman, G. B., Roehl, C., Wennberg, P. O., and Wunch, D.: The Orbiting Carbon Observatory
- 10 (OCO-2): spectrometer performance evaluation using pre-launch direct sun measurements, *Atmos. Meas. Tech.*, 8, 301–313, doi:10.5194/amt-8-301-2015, 2015.
- Garny, H., Dameris, M., Randel, W., Bodeker, G. E., and Deckert, R.: Dynamically forced increase of tropical upwelling in the lower stratosphere, *J. Atmos. Sci.*, 68, 1214–1233, doi:10.1175/2011JAS3701.1, 2011.
- 15 Gettelman, A., Hoor, P., Pan, L. L., Randel, W. J., Hegglin, M. I., and Birner, T.: The extratropical upper troposphere and lower stratosphere, *Rev. Geophys.*, 49, doi:10.1029/2011RG000355, 2011.
- Gurk, C., Fischer, H., Hoor, P., Lawrence, M. G., Lelieveld, J., and Wernli, H.: Airborne in-situ measurements of vertical, seasonal and latitudinal distributions of carbon dioxide over Europe, *Atmos. Chem. Phys.*, 8, 6395–6403, 2008.
- 20 Hammerling, D. M., Michalak, A. M., O’Dell, C., and Kawa, S. R.: Global CO₂ distributions over land from the Greenhouse Gases Observing Satellite (GOSAT), *Geophys. Res. Lett.*, 39, doi:10.1029/2012GL051203, 2012.
- Haynes, P. H. and Shuckburgh, E.: Effective diffusivity as a diagnostic of atmospheric transport 1. Stratosphere, *J. Geophys. Res.*, 105, 22,777–22,794, doi:10.1029/2000JD900093, 2000a.
- 25 Haynes, P. H. and Shuckburgh, E.: Effective diffusivity as a diagnostic of atmospheric transport 2. Troposphere and lower stratosphere, *J. Geophys. Res.*, 105, 22 795–22 810, doi:10.1029/2000JD900092, 2000b.
- Hegglin, M. I., Brunner, D., Peter, T., Staehelin, J., Wirth, V., Hoor, P., and Fischer, H.: Determination of eddy diffusivity in the lowermost stratosphere, *Geophys. Res. Lett.*, 32, L13 812, doi:10.1029/2005GL022495, 2005.
- 30 Hegglin, M. I., Boone, C. D., Manney, G. L., Shepherd, T. G., Walker, K. A., Bernath, P. F., Daffer, W. H., Hoor, P., and Schiller, C.: Validation of ACE-FTS satellite data in the upper troposphere/lower stratosphere (UTLS) using non-coincident measurements, *Atmospheric Chemistry and Physics*, 8,



- 1483–1499, doi:10.5194/acp-8-1483-2008, <http://www.atmos-chem-phys.net/8/1483/2008/>, 2008.
- Hegglin, M. I., Gettelman, A., Hoor, P., Krichevsky, R., Manney, G. L., Pan, L. L., Son, S.-W., Stiller, G., Tilmes, S., Walker, K. A., Eyring, V., Shepherd, T. G., Waugh, D., Akiyoshi, H., J. A. A., Austin, J., Baumgaertner, A., Bekki, S., Braesicke, P., Brühl, C., Butchart, N., Chipperfield, M., Dameris, M., Dhomse, S., Frith, S., Garny, H., Hardiman, S. C., Jöckel, P., Kinnison, D. E., Lamarque, J. F., Mancini, E., Michou, M., Morgenstern, O., Nakamura, T., Olivié, D., Pawson, S., Pitari, G., Plummer, D. A., Pyle, J. A., Rozanov, E., Scinocca, J. F., Shibata, K., Smale, D., Teyssédre, H., Tian, W., and Yamashita, Y.: Multimodel assessment of the upper troposphere and lower stratosphere: Extratropics, *J. Geophys. Res.*, 115, D00M09, doi:10.1029/2010JD013884, 2010.
- 10 Holton, J. R., Haynes, P. H., McIntyre, M. E., Douglass, A. R., Rood, R. B., and Pfister, L.: Stratosphere-troposphere exchange, *Rev. Geophys.*, 33, 403–440, doi:10.1029/95RG02097, 1995.
- Hoor, P., Gurk, C., Brunner, D., Hegglin, M. I., Wernli, H., and Fischer, H.: Seasonality and extent of extratropical TST derived from in-situ CO measurements during SPURT, *Atmos. Chem. Phys.*, 4, 1427–1442, 2004.
- 15 Hoor, P., Fischer, H., and Lelieveld, J.: Tropical and extratropical tropospheric air in the lowermost stratosphere over Europe: A CO-based budget, *Geophys. Res. Lett.*, 32, L13 812, doi:10.1029/2005GL022495, 2005.
- Hoor, P., Wernli, H., Hegglin, M. I., and Bönisch, H.: Transport timescales and tracer properties in the extratropical UTLS, *Atmospheric Chemistry and Physics*, 10, 7929–7944, doi:10.5194/acp-10-7929-2010, <http://www.atmos-chem-phys.net/10/7929/2010/>, 2010.
- 20 James, R. and Legras, B.: Mixing processes and exchanges in the tropical and the subtropical UT/LS, *Atmos. Chem. Phys.*, 9, 25–38, doi:10.5194/acp-9-25-2009, 2009.
- Koh, T.-Y. and Legras, B.: Hyperbolic lines and the stratospheric polar vortex, *AIP, Chaos: An Interdisciplinary Journal of Nonlinear Science*, 12, doi:10.1063/1.1480442, 2002.
- 25 Konopka, P., Grooß, J.-U., Günther, G., McKenna, D. S., Müller, R., Elkins, J., Fahey, D., and Popp, P.: Weak impact of mixing on chlorine deactivation during SOLVE/THESEO 2000: Lagrangian modeling (CLaMS) versus ER-2 in situ observations, *J. Geophys. Res.*, 108(D5), 8324, doi:10.1029/2001JD000876, 2003.
- Lacis, A. A., Wuebbles, D. J., and Logan, J. A.: Radiative forcing of climate by changes in the vertical distribution of ozone, *J. Geophys. Res.*, 95, 9971–9981, doi:10.1029/JD095iD07p09971, 1990.
- 30 Legras, B., Joseph, B., and Lefèvre, F.: Vertical diffusivity in the lower stratosphere from Lagrangian back-trajectory reconstructions of ozone profiles, *J. Geophys. Res.*, 108, 4562, doi:10.1029/2002JD003045, 2003.



- Legras, B., Pisso, I., Berthet, G., and Lefèvre, F.: Variability of the Lagrangian turbulent diffusion in the lower stratosphere, *Atmos. Chem. Phys.*, 5, 1605–1622, doi:10.5194/acp-5-1605-2005, 2005.
- Li, F., Waugh, D. W., Douglass, A. R., Newman, P. A., Pawson, S., Stolarski, R. S., Strahan, S. E., and Nielsen, J. E.: Seasonal variations of stratospheric age spectra in the Goddard Earth Observing System Chemistry Climate Model (GEOSCCM), *J. Geophys. Res.*, 117, doi:10.1029/2011JD016877, 2012.
- Li, S. and Waugh, D. W.: Sensitivity of mean age and long-lived tracers to transport parameters in a two-dimensional model, *J. Geophys. Res.*, 104, 30 559–30 569, doi:10.1029/1999JD900913, 1999.
- Liu, J., Bowman, K. W., and Henze, D. K.: Source-receptor relationships of column-average CO₂ and implications for the impact of observations on flux inversions, *J. Geophys. Res.*, 120, 5214–5236, doi:10.1002/2014JD22914, 2014.
- Miyazaki, K., T. M., Patra, P. K., Sawa, Y., Matsueda, H., and Nakazawa, T.: Formation mechanisms of latitudinal CO₂ gradients in the upper troposphere over the subtropics and tropics, *J. Geophys. Res.*, 114, 2009.
- Nakamura, N., Miyashita, K., Aoki, S., and Tanaka, M.: Temporal and spatial variation of upper tropospheric and lower stratospheric carbon dioxide, *Tellus*, 43B, 106–117, 1991.
- Olsen, S. C. and Randerson, J. T.: Differences between surface and column atmospheric CO₂ and implications for carbon cycle research, *J. Geophys. Res.*, 109, doi:10.1029/2003JD003968, 2004.
- Pan, L. L., Konopka, P., and Browell, E. V.: Observations and model simulations of mixing near the extratropical tropopause, *J. Geophys. Res.*, 111, D05 106, doi:10.1029/2005JD006480, 2006.
- Park, M., Randel, W. J., Gettelman, A., Massie, S. T., and Jiang, J. H.: Transport above the Asian summer monsoon anticyclone inferred from aura microwave limb sounder tracers, *J. Geophys. Res.*, 112, doi:10.1029/2006JD008294, 2007b.
- Park, M., Randel, W. J., Emmons, L. K., Bernath, P. F., Walker, K. A., and Boone, C. D.: Chemical isolation in the Asian monsoon anticyclone observed in Atmospheric Chemistry Experiment (ACE-FTS) data, *Atmos. Chem. Phys.*, 8, 757–764, doi:10.5194/acp-8-757-2008, 2008.
- Park, M., Randel, W. J., Emmons, L. K., and Livesey, N. J.: Transport pathways of carbon monoxide in the Asian summer monsoon diagnosed from Model of Ozone and Related Tracers (MOZART), *J. Geophys. Res.*, 114, D08 303, doi:10.1029/2008JD010621, 2009.
- Park, S., Jimenez, R., Daube, B. C., Pfister, L., Conway, T. J., Gottlieb, E. W., Chow, V. Y., Curran, D. J., Matross, D. M., Bright, A., Atlas, E. L., Bui, T. P., Gao, R.-S., Twohy, C. H., and Wofsy, S. C.: The CO₂ tracer clock for the Tropical Tropopause Layer, *Atmos. Chem. Phys.*, 7, 3989–4000, doi:10.5194/acp-7-3989-2007, 2007a.



- 5 Park, S., Atlas, E. L., Jiménez, R., Daube, B. C., Gottlieb, E. W., Nan, J., Jones, D. B. A., Pfister, L., Conway, T. J., Bui, T. P., Gao, R.-S., and Wofsy, S. C.: Vertical transport rates and concentrations of OH and Cl radicals in the Tropical Tropopause Layer from observations of CO₂ and halocarbons: implications for distributions of long- and short-lived chemical species, *Atmos. Chem. Phys.*, 10, 6669–6684, doi:10.5194/acp-10-6669-2010, 2010.
- Peters, W., Jacobson, A. R., Sweeney, C., Andrews, A. E., Conway, T. J., Masarie, K., Miller, J. B., Bruhwiler, L. M. P., Petron, G., Hirsch, A. I., Worthy, D. E. J., van der Werf, G. R., Randerson, J. T., Wennberg, P. O., Krol, M. C., and Tans, P. P.: An atmospheric perspective on North American carbon dioxide exchange: CarbonTracker, *Proceed. Nat. Acad. Sc.*, 104, 18 925–18 930, 2007.
- 10 Pisso, I. and Legras, B.: Turbulent vertical diffusivity in the sub-tropical stratosphere, *Atmos. Chem. Phys.*, 8, 697–707, 2008.
- Pommrich, R., Müller, R., Grooß, J.-U., Konopka, P., Ploeger, F., B. Vogel, M. T., Hoppe, C. M., Günther, G., Spelten, N., Hoffmann, L., Pumphrey, H.-C., S. Viciani, F. D., Volk, C. M., Hoor, P., Schlager, H., and Riese, M.: Tropical troposphere to stratosphere transport of carbon monoxide and long-lived trace species in the Chemical Lagrangian Model of the Stratosphere (CLaMS), *Geosci. Model Dev.*, 7, 2895–2916, doi:10.5194/gmd-7-2895-2014, 2014.
- 15 Randel, W. J., Park, M., Wu, F., and Livesey, N.: Asian monsoon transport of pollution to the stratosphere, *Science*, 328(5978), 611–613, doi:10.1126/science.1182274, 2010.
- Ray, E. A., Moore, F. L., Rosenlof, K. H., Davis, S. M., Sweeney, C., Bönisch, H., Engel, A., Sugawara, S., Nakazawa, T., and Aoki, S.: Improving stratospheric transport trend analysis based on SF₆ and CO₂ measurements, *J. Geophys. Res.*, 119, 14 110–14 128, doi:10.1002/2014JD021802, 2014.
- 20 Riese, M., Ploeger, F., Rap, A., Vogel, B., Konopka, P., Dameris, M., and Forster, P.: Impact of uncertainties in atmospheric mixing on simulated UTLS composition and related radiative effects, *J. Geophys. Res.*, 117, D16305, doi:10.1029/2012JD017751, 2012.
- 25 Salby, M. L. and Callaghan, P. F.: Interaction between the Brewer Dobson Circulation and the Hadley Circulation, *Journal of Climate*, 18, 4303–4316, doi:10.1175/JCLI3509.1, 2005.
- Salby, M. L. and Callaghan, P. F.: Influence of the Brewer-Dobson circulation on stratosphere-troposphere exchange, *J. Geophys. Res.*, 111, D21106, doi:10.1029/2006JD007051, 2006.
- Sawa, Y., Machida, T., and Matsueda, H.: Seasonal variations of CO₂ near the tropopause observation by commercial aircraft, *J. Geophys. Res.*, 113, 2008.
- 30 Sawa, Y., Machida, T., and Matsueda, H.: Aircraft observation of the seasonal variation in the transport of CO₂ in the upper atmosphere, *J. Geophys. Res.*, 117, 2012.
- Scheele, M., Siegmund, P., and van Velthoven, P.: Stratospheric age of air computed with trajectories



- based on various 3D-Var and 4D-Var data sets, *Atmos. Chem. Phys.*, 5, 1–7, 2005.
- Schuck, T. J., Brenninkmeijer, C. A. M., Slemr, F., Xueref-Remy, I., and Zahn, A.: Greenhouse gas analysis of air samples collected onboard the CARIBIC passenger aircraft, *Atmos. Meas. Tech.*, 2, 449–464, doi:10.5194/amt-2-449-2009, <http://www.atmos-meas-tech.net/2/449/2009/>, 2009.
- 5 Shia, R.-L., Liang, M.-C., Miller, C. E., and Yung, Y. L.: CO₂ in the upper troposphere: Influence of stratosphere-troposphere exchange, *Geophys. Res. Lett.*, 33, doi:10.1029/2006GL026141, 2006.
- Sprung, D. and Zahn, A.: Acetone in the upper troposphere/lowermost stratosphere measured by the CARIBIC passenger aircraft: Distribution, seasonal cycle, and variability, *J. Geophys. Res.*, 115, doi:10.1029/2009JD012099, 2010.
- 10 Stohl, A., Forster, C., Frank, A., Seibert, P., and Wotawa, G.: Technical note: The Lagrangian particle dispersion model FLEXPART version 6.2, *Atmos. Chem. Phys.*, 5, 2461–2474, doi:10.5194/acp-5-2461-2005, 2005.
- Strahan, S., Douglass, A., Nielsen, J. E., and Boering, K. A.: The CO₂ seasonal cycle as a tracer of transport, *J. Geophys. Res.*, D12, 13,729–13,741, doi:10.1029/98JD01143, 1998.
- 15 Strahan, S. E., Duncan, B. N., and Hoor, P.: Observationally derived transport diagnostics for the lowermost stratosphere and their application to the GMI chemistry and transport model, *Atmospheric Chemistry and Physics*, 7, 2435–2445, doi:10.5194/acp-7-2435-2007, <http://www.atmos-chem-phys.net/7/2435/2007/>, 2007.
- Tans, P. P. and Keeling, R.: Trends in atmospheric carbon dioxide, NOAA-ERSL webpage, 2015.
- 20 Waugh, D.: Atmospheric dynamics: The age of stratospheric air, *Nature Geoscience*, 2, 14–16, doi:10.1038/ngeo397, 2009.
- Waugh, D. and Hall, T.: Age of stratospheric air: Theory, observations, and models, *Rev. Geophys.*, 40, 1010, doi:10.1029/2000RG000101, 2002.
- 25 Worden, J., Noone, D., Galewsky, J., Bailey, A., Bowman, K., Brown, D., Hurley, J., Kulawik, S., Lee, J., and Strong, M.: Analysis based on data submitted by November 2014, except for the greenhouse gas species CO₂, CH₄, N₂O, SF₆ and halocarbons, for which the submission period ended in July 2014, WDCGG report, p. 130 pp., 2015.

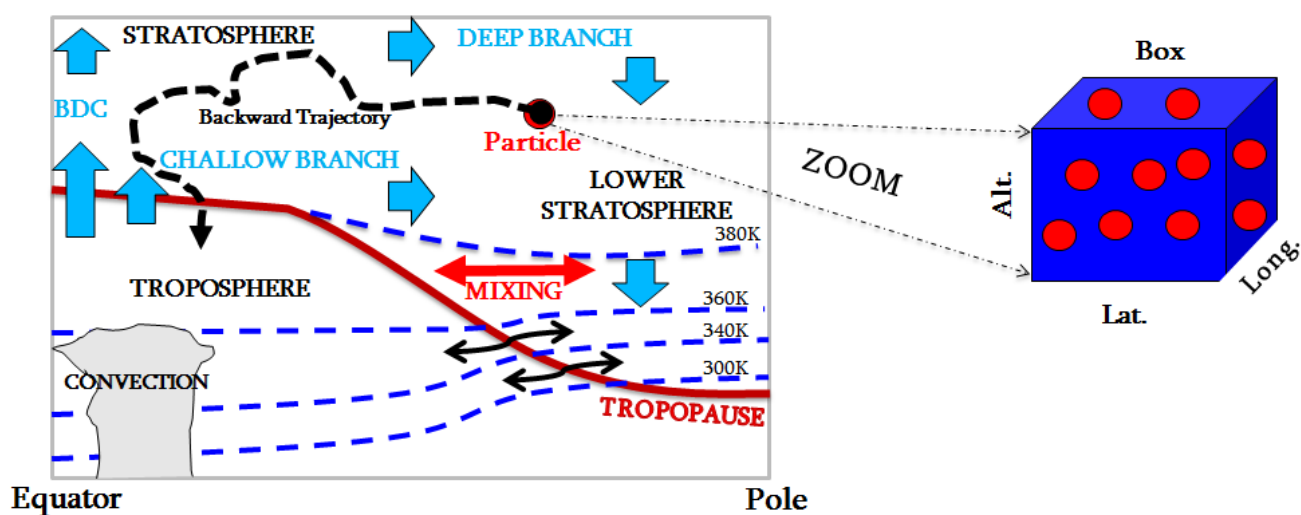


Fig. 1: A schematic representation of the initialization of air particles in the (latitude \times longitude \times altitude) grid box for the integration of backward trajectories.

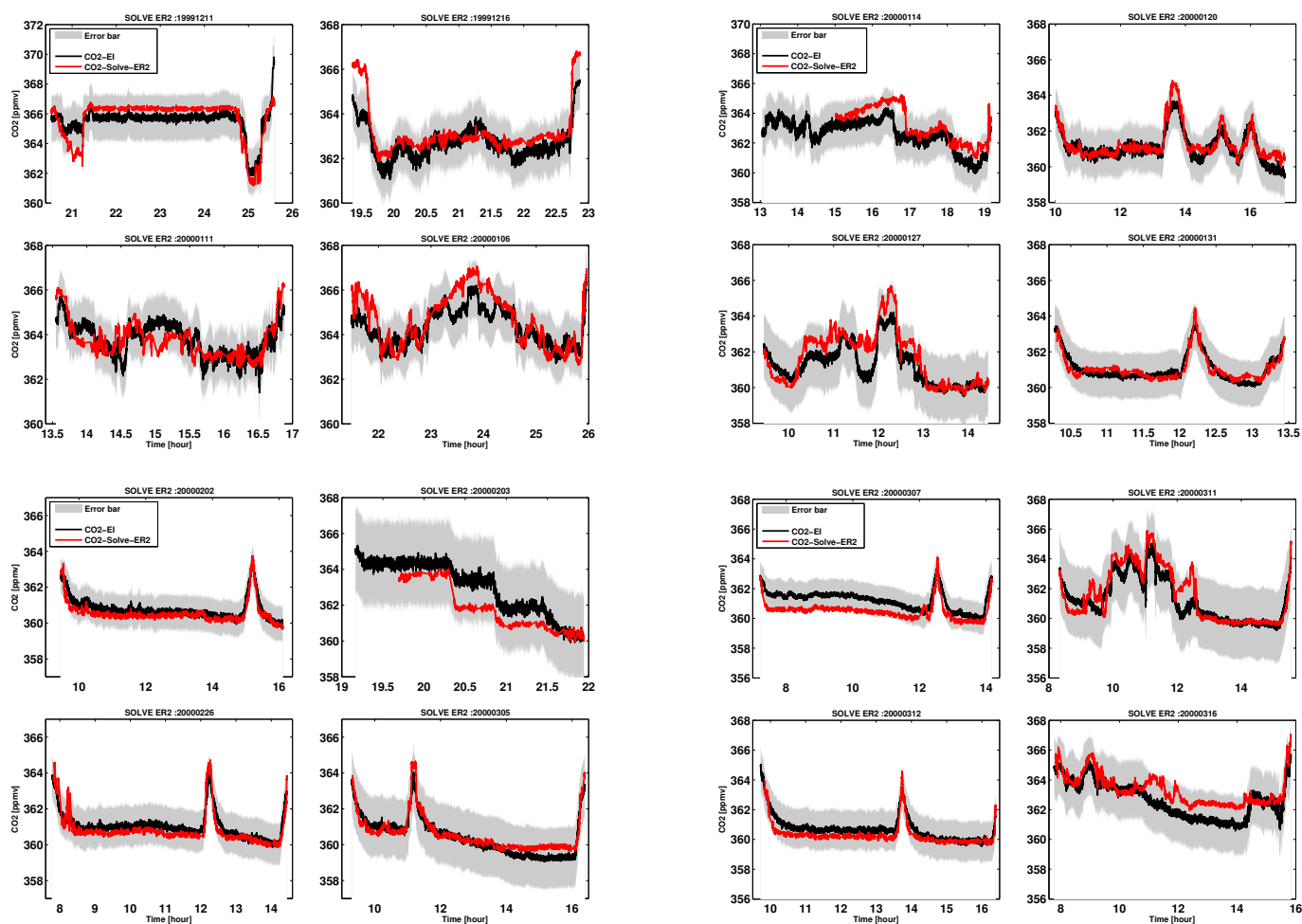


Fig. 2: Comparison between CO_2 calculated from backward trajectories and those from aircraft measurements during SOLVE campaign (Daube et al., 2002). (Black): reconstructed CO_2 along the ER-2 flight track by the Lagrangian transport model. (Red): observed CO_2 .

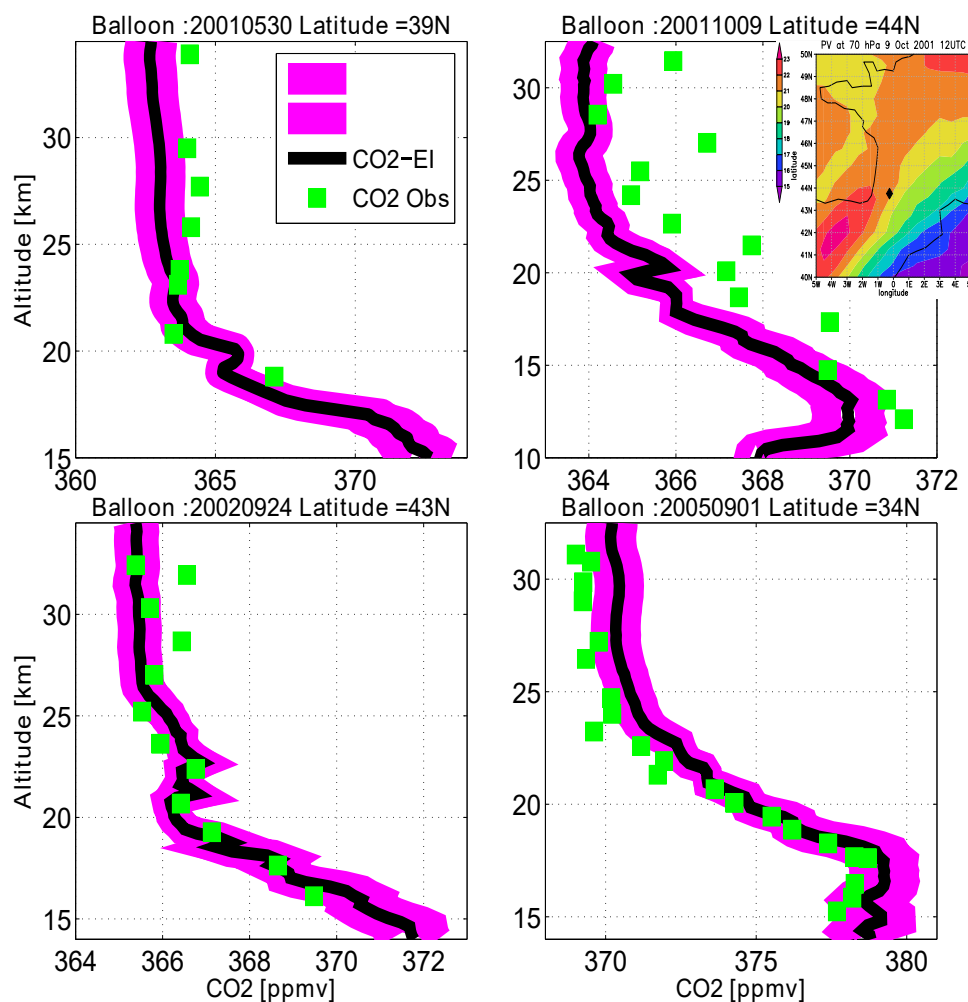


Fig. 3: Reconstructed vertical profiles of the mean CO_2 compared with those from each *in situ* stratospheric balloon observations of CO_2 (Engel et al., 2009). (Black curves): vertical profiles of mean diabatic CO_2 . (Green square): *in situ* balloon measurements of CO_2 . The measurements were taken from Sanriku, Japan (39.33°N) on 30 May 2001, Aire sur l'Adour, France (43.75°N) on 24 September 2002 and on 9 October 2001 and Ft. Sumner, New Mexico, USA (34.5°N) on 17 September 2004, respectively. The insert on the upper right panel shows the potential vorticity (in PVU) on the 70 hPa surface for 9 October 2001 at 12UTC over France from ERA-Interim. The location of Aire sur l'Adour is indicated by a diamond.

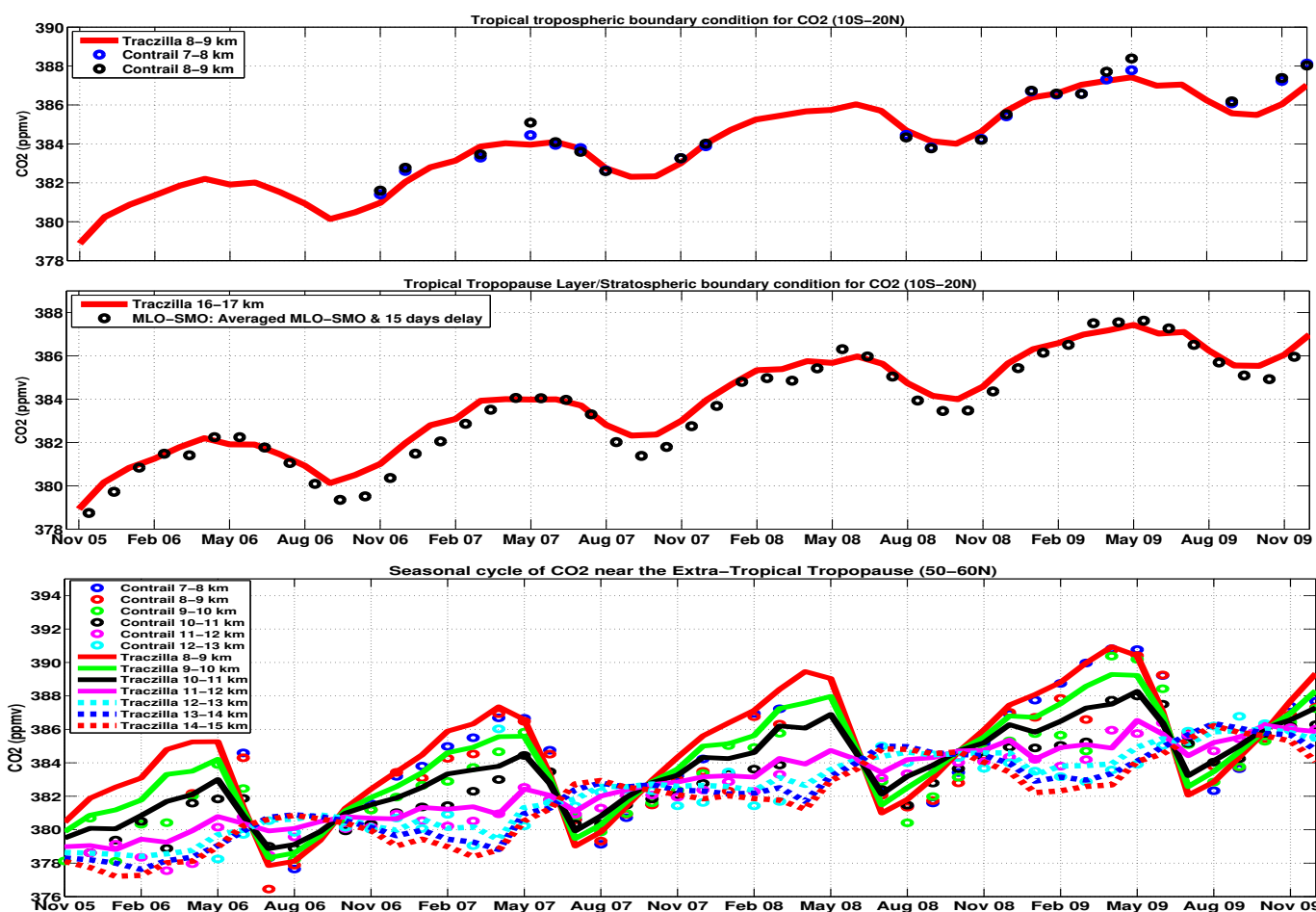


Fig. 4: Evolution of the monthly mean CO_2 seasonal cycle from TRACZILLA calculations (line) compared with those derived from CONTRAIL measurements (circle). (Top): Tropospheric boundary condition for TRACZILLA CO_2 averaged from 10°S – 20°N and compared with CONTRAIL measurements for the same time period and latitude bin. (Mid): Stratospheric boundary condition for TRACZILLA CO_2 averaged from 10°S – 20°N and compared with the average of surface station data from Mauna Loa, Hawaii (19°N) and American Samoa (14°S) delayed by 15 days (Andrews et al., 2001a). (Bottom): Comparison of the CO_2 seasonal cycle from TRACZILLA with CONTRAIL near extra-tropical tropopause at 50 – 60°N and at several heights from 7 to 15 km over the same time period from November 2005 to January 2010 (see Sawa et al. (2008) for CONTRAIL data).

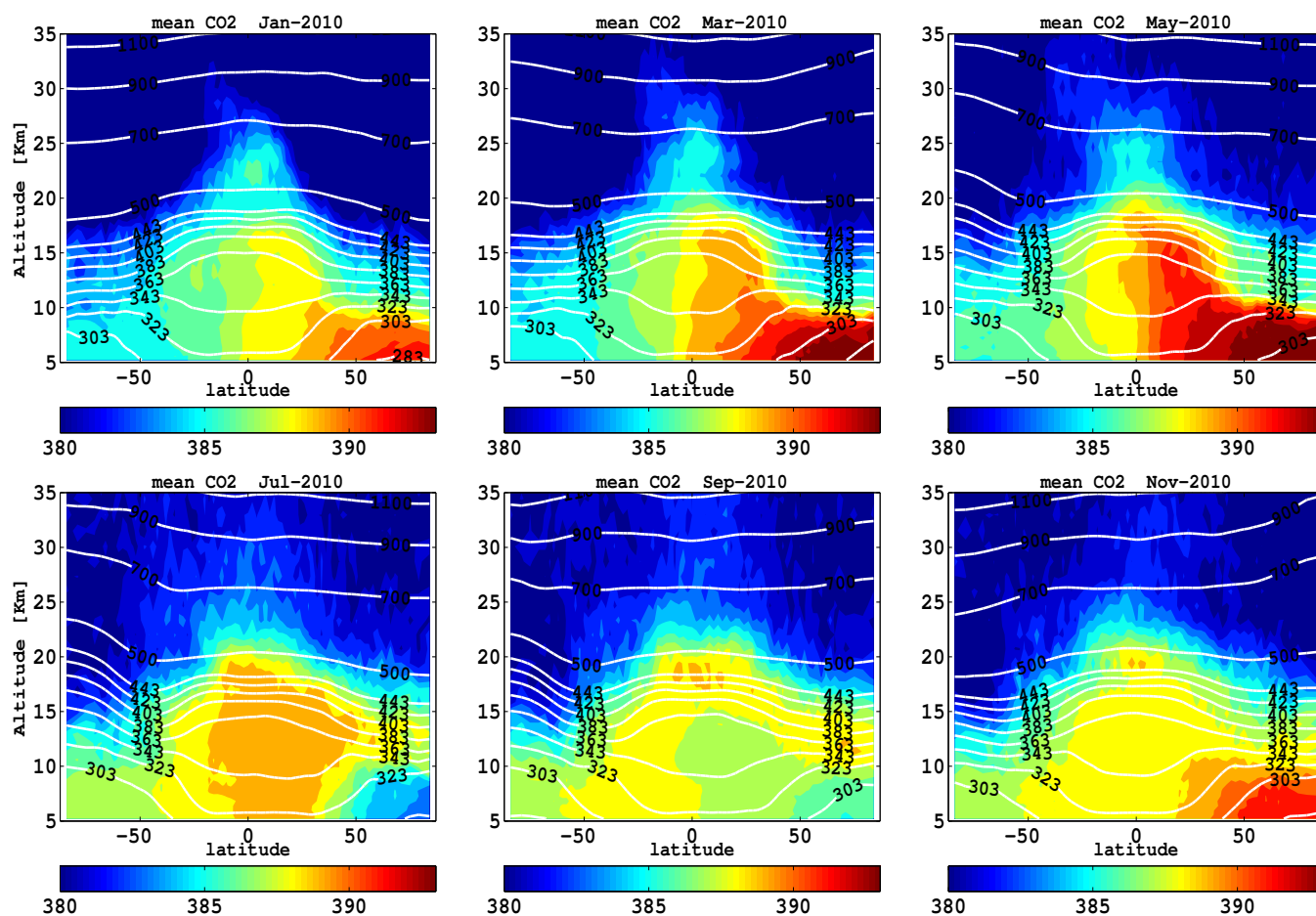


Fig. 5: Global distribution of the seasonal cycle of the mean CO₂ (in ppmv) from the free troposphere to the stratosphere shown as latitude-altitude cross sections for January, March, May, July, September and November of the year 2010. The white lines indicate the isentropic surface levels for each given month.

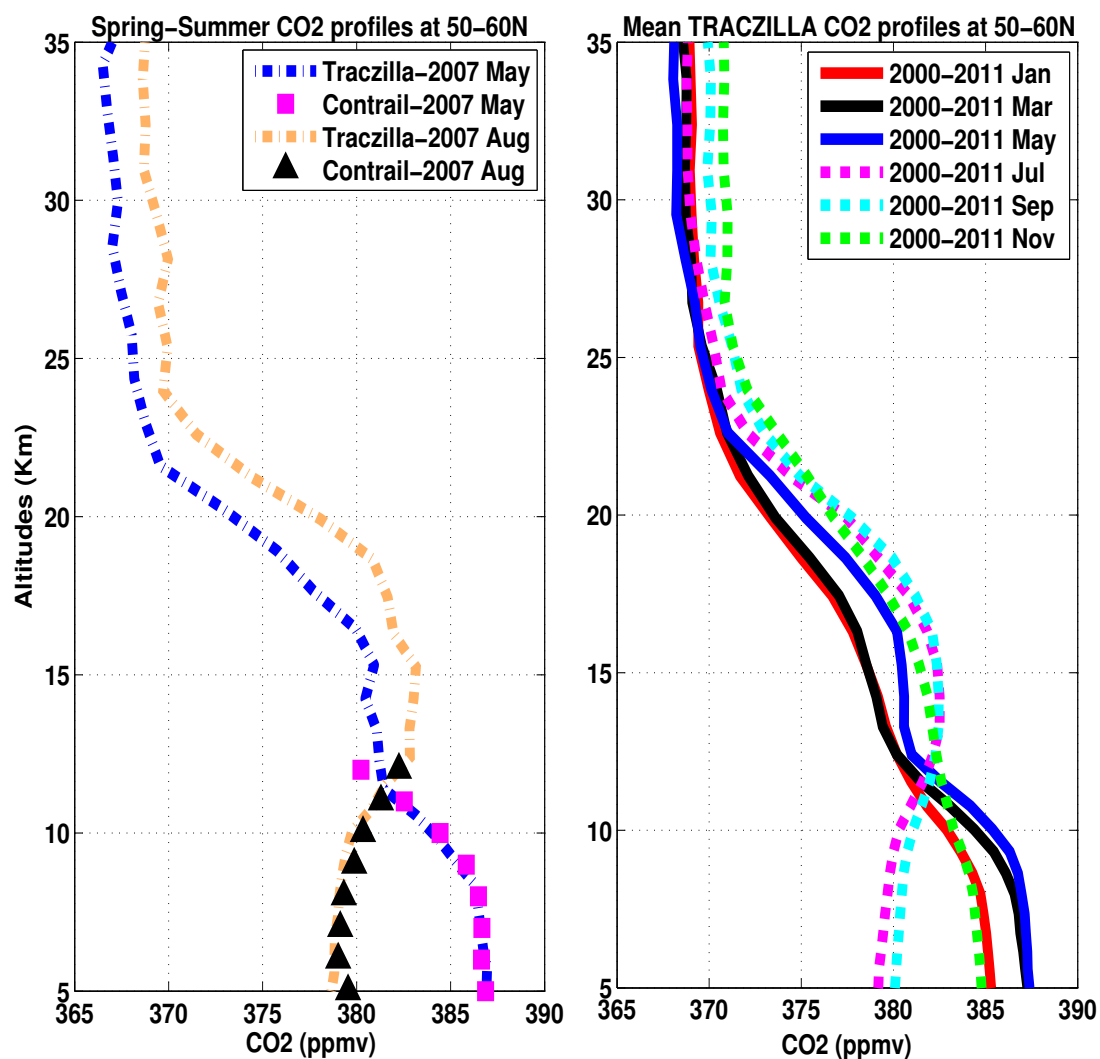


Fig. 6: Reconstructed vertical profiles of the mean CO₂ compared with those from CONTRAIL aircraft measurements for 2007 at 50-60°N (Left). Averaged monthly profiles of the reconstructed CO₂ over the period 2000-2010 after removal of the mean CO₂ trend at each level and centered on 2007. Left: (Dotted-dashed lines): vertical profiles of CO₂ from TRACZILLA (blue: May, orange: Aug). (Symbols): *in situ* aircraft measurements from CONTRAIL campaign (magenta square: May, orange triangle: Aug). Right: monthly vertical profiles from TRACZILLA (January (red), March (black), May (blue), July (magenta), September (cyan) and November (green)).